

Alkane and Alkanethiol Passivation of Halogenated Ge Nanowires

Gillian Collins,^{†,‡} Peter Fleming,^{†,‡} Sven Barth,^{†,‡} Colm O'Dwyer,[‡] John J. Boland,^{‡,§}
Michael A. Morris,^{†,‡} and Justin D. Holmes^{*,†,‡}

[†]Materials and Supercritical Fluids Group, Department of Chemistry and the Tyndall National Institute, University College Cork, Cork, Ireland, [‡]Centre for Research on Adaptive Nanostructures and Nanodevices (CRANN), and [§]School of Chemistry, Trinity College Dublin, Dublin 2, Ireland, and [‡]Department of Physics and Materials and Surface Science Institute, University of Limerick, Limerick, Ireland

Received August 20, 2010. Revised Manuscript Received October 28, 2010

The ambient stability and surface coverage of halogen (Cl, Br, and I) passivated germanium nanowires were investigated by X-ray photoelectron and X-ray photoelectron emission spectroscopy. After exposure to air for 24 h, the stability of the halogen-terminated Ge nanowire surfaces toward reoxidation was found to improve with the increasing size of the halogen atoms, i.e., $I > Br > Cl$. Halogen termination was effective in removing the native Ge oxide (GeO_x) and could also be utilized for further functionalization. Functionalization of the halogenated Ge nanowires was investigated using alkyl Grignard reagents and alkanethiols. The stability of the alkyl and alkanethiol passivation layers from the different halogen-terminated surfaces was investigated by X-ray photoelectron spectroscopy and attenuated total reflectance infrared spectroscopy. Alkanethiol functionalized nanowires showed greater resistance against reoxidation of the Ge surface compared to alkyl functionalization when exposed to ambient conditions for 1 week.

Introduction

Group 14 semiconductor nanowires have been successfully fabricated via several different bottom-up and top-down strategies.¹ Germanium (Ge) offers potential advantages over silicon (Si) for performance gains in high speed electronic devices due to greater free carrier mobility.^{2,3} There have been advances in Ge nanowire growth, and several groups have already demonstrated the fabrication of single Ge nanowire devices such as field effect transistors (FETs)^{4–6} and p – n junctions.⁷ However, Ge possesses an unstable, nonuniform oxide surface on both bulk and nanowire surfaces which gives rise to a poor Ge/GeO_x interface characterized by a high density of surface states.^{8,9} The negative influence of these surface states on the electrical properties of nanowires has been

theoretically and experimentally studied.^{10–13} The successful integration of Ge nanowires into many device applications consequently requires effective surface oxide removal and passivation. Literature studies have shown the oxidation of Ge surfaces to be a complex process depending on the conditions such as a wet or dry environment, illumination, and crystal orientation.^{14,15} Using high resolution X-ray photoelectron spectroscopy (XPS), Schmeisser et al.¹⁶ could resolve all four oxidation states in the Ge 3d spectrum and found a core level shift of 0.85 eV per oxidation state. Unlike Si, which exhibits only one stable oxide (SiO_2), Ge forms stable oxides in the 2+ (GeO) and 4+ (GeO_2) oxidation states, the latter being soluble in water. Prabhakaran and Ogino¹⁷ found that bulk single crystal surfaces of Ge oxidized in a dry O_2 environment, forming predominately Ge^{2+} , while exposure to ambient conditions led to a mixture of oxides, mainly Ge^{2+} and Ge^{4+} , proposing that atmospheric moisture plays a role in the formation of higher Ge oxidation states. Furthermore, the oxidation species observed on nanowire surfaces differs from those reported on bulk planar Ge surfaces, for example, thermal annealing of air-oxidized bulk Ge favors the formation of the 2+ species,¹⁶

*To whom correspondence should be addressed. Tel: +353(0)21 4903608. Fax: +353 (0)21 4274097. E-mail: j.holmes@ucc.ie.

- (1) Barth, S.; Hernandez-Ramirez, F.; Holmes, J. D.; Romano-Rodriguez, A. *Prog. Mater. Sci.* **2010**, 55(6), 563.
- (2) Yu, B.; Sun, X. H.; Calebotta, G. A.; Dholakia, G. R.; Meyyappan, M. J. *Cluster Sci.* **2006**, 17(4), 579.
- (3) Bandaru, P. R.; Pichanusakorn, P. *Semicond. Sci. Technol.* **2010**, 25, 024003.
- (4) Greytak, A. B.; Lauhon, L. J.; Gudiksen, M. S.; Lieber, C. M. *Appl. Phys. Lett.* **2004**, 84(21), 4176.
- (5) Saraswat, K. C.; Chui, C. O.; Krishnamohan, T.; Nayfeh, A.; McIntyre, P. *Microelectron. Eng.* **2005**, 80, 15.
- (6) Wang, D. W.; Chang, Y. L.; Wang, Q.; Cao, J.; Farmer, D. B.; Gordon, R. G.; Dai, H. J. *J. Am. Chem. Soc.* **2004**, 126(37), 11602.
- (7) Tutuc, E.; Appenzeller, J.; Reuter, M. C.; Guha, S. *Nano Lett.* **2006**, 6(9), 2070.
- (8) Afanas'ev, V. V.; Fedorenko, Y. G.; Stesmans, A. *Appl. Phys. Lett.* **2005**, 87(3).
- (9) Houssa, M.; Chagarov, E.; Kummel, A. *MRS Bull.* **2009**, 34, 504.
- (10) Hanrath, T.; Korgel, B. A. *J. Phys. Chem. B* **2005**, 109(12), 5518.
- (11) Medaboina, D.; Gade, V.; Patil, S. K. R.; Khare, S. V. *Phys. Rev. B* **2007**, 76, 205327.

- (12) Voon, L. C. L. Y.; Zhang, Y.; Lassen, B.; Willatzen, M.; Xiong, Q.; Eklund, P. C. *J. Nanosci. Nanotechnol.* **2008**, 8, 1.
- (13) Prasankumar, R. P.; Choi, S.; Trugman, S. A.; Picraux, S. T.; Taylor, A. J. *Nano Lett.* **2008**, 8(6), 1619.
- (14) Tabet, N.; Faiz, M.; Hamdan, N. M.; Hussain, Z. *Surf. Sci.* **2003**, 523, 68.
- (15) Sun, S.; Sun, Y.; Liu, Z.; Lee, D.; Pianetta, P. *Appl. Phys. Lett.* **2006**, 89, 231925.
- (16) Schmeisser, D.; Schnell, R. D.; Bogen, A.; Himpsel, F. J.; Rieger, D. *Surf. Sci.* **1986**, 172, 455.
- (17) Prabhakaran, K.; Ogino, T. *Surf. Sci.* **1995**, 325, 263.

while thermal annealing of water-oxidized Ge nanowires results predominately in the formation of the 1+ oxide.¹⁸ This difference in oxidizing behavior is most likely due to the high curvature of the nanowire surfaces. Removal of the surface oxide, GeO_x, is typically achieved by treatment with aqueous HF solution, resulting in hydrogen-terminated surfaces.¹⁹ The stability of the H-passivation layer on Ge surfaces is limited to a few minutes when exposed to ambient conditions.²⁰

Termination of Ge surfaces with halogens was first achieved by Cullen et al.²¹ using hot gaseous HCl. Since then, milder passivation methods including dilute halide acids (HCl, HBr, and HI) and electrochemical dissociation of silver halide salts under ultra high vacuum conditions have proved effective for Cl, Br, and I passivation of Ge.^{22–24} Sun and co-workers²⁵ detected the presence of both monochloride and dichloride species on HCl treated bulk Ge(100) surfaces, while the Ge(111) surface was found to be terminated only by the monochloride which was attributed to the Ge(111) surface having only one dangling bond. They further observed that HF treatment resulted in greater surface roughness compared to HCl treatment due to the greater Ge back-bond breaking that occurs with HF etching.²⁵ In a later paper, Sun et al.¹⁵ investigated the oxidation behavior of Cl- and Br-terminated surfaces and illustrated three important findings: (i) Cl/Br-terminated surfaces displayed increased resistance to reoxidation relative to H surfaces under dry conditions, (ii) the presence of water vapor resulted in the halogen species being replaced by –OH groups, which allowed easier oxidative attack by atmospheric O₂ and water vapor, due to the smaller size of the –OH groups, and (iii) the rate of surface oxidation was greatly enhanced by the presence of UV light. While these and other reports^{20,26–28} have been conducted on bulk single crystal Ge, Adhikari and co-workers²⁹ carried out XPS studies of HF- and HCl-treated Ge nanowires with synchrotron radiation and found similar stability trends, i.e., chlorinated surfaces displayed an increased stability relative to H-terminated surfaces. To date, Ge nanowire passivation with heavier halogens (Br and I termination) has been reported by Jagannathan et al.³⁰

Hydrogen and halogenated surfaces can also be subsequently employed as further scaffolds for the attachment of organic ligands. Unsaturated hydrocarbons have previously been grafted onto H-terminated Si and Ge surfaces.^{31–34} These hydrosilylation and hydrogermylation reactions can be achieved by thermal activation, UV initiation, or Lewis acid mediation.^{35–38} The attachment of alkyl chains has been demonstrated on Cl-terminated surfaces using Grignard reagents. This chlorination/alkylation route has been effective for functionalizing both bulk^{39,40} and nanowire^{41,42} surfaces of Si and Ge. Ge surfaces passivated with alkyl chains show far greater stability compared to hydrogen or halogenated (Cl/Br/I) surfaces due to the strong Ge–C bond (460 kJ mol^{–1}) and the presence of a hydrophobic monolayer hindering the access of oxidizing species toward the Ge surface. Functionalization of Ge with alkanethiols is typically achieved via hydrogen passivated surfaces,^{43–45} but Bent and co-workers⁴⁶ found that alkanethiol passivation could also be achieved on planar Cl- and Br-terminated surfaces.

Here, we present a detailed investigation into the relative stability of Cl-, Br-, and I-terminated Ge nanowires using XPS. While previous studies on Ge nanowire passivation have focused on nanowire bundles, we utilize X-ray photoelectron emission microscopy (XPEEM) to analyze individual Br- and I-terminated Ge nanowire surfaces. We compare the reactivity of these halogenated surfaces toward further functionalization with Grignard reagents and alkanethiols. We further evaluate the effectiveness of alkane and alkanethiol passivation layers, obtained from different halogenated Ge surfaces, to prevent the reoxidation of Ge nanowires.

Experimental Section

Ge Nanowire Synthesis and Passivation. The Ge nanowires used in this study were synthesized by the thermal decomposition of diphenylgermane (purchased from ABCR, Germany) in the presence of gold-coated silicon substrates in supercritical (sc) toluene. Details of the experimental setup have been described elsewhere.⁴⁷

- (18) Hanrath, T.; Korgel, B. A. *J. Am. Chem. Soc.* **2004**, *126*, 15466.
- (19) Zhang, R. Q.; Zhao, Y. L.; Teo, B. K. *Phys. Rev. B* **2004**, *69*, 125319.
- (20) Rivillon, S.; Chabal, Y. J.; Amy, F.; Kahn, A. *Appl. Phys. Lett.* **2005**, *87*, 253101.
- (21) Cullen, G. W.; Amick, J. A.; Gerlich, D. *J. Electrochem. Soc.* **1962**, *109*, 124.
- (22) Kim, J.; Liu, S.; Tan, S.; McVittie, J.; Saraswat, K.; Nishi, Y. *ECS Trans.* **2006**, *3*(7), 1191.
- (23) Forchier, M.; McEllistrem, M. T.; Boland, J. J. *Surf. Sci.* **1997**, *385*, L905.
- (24) Gothelid, M.; LeLay, G.; Wigren, C.; Bjorkqvist, M.; Karlsson, U. O. *Surf. Sci.* **1997**, *371*, 264.
- (25) Sun, Y.; Liu, Z. L.; D.; Peterson, S.; Pianetta, P. *Appl. Phys. Lett.* **2006**, *88*, 021903.
- (26) Bodlaki, D.; Yamamoto, H.; Waldeck, D. H.; Borguet, E. *Surf. Sci.* **2003**, *543*, 63.
- (27) Lu, Z. H. *Appl. Phys. Lett.* **1996**, *68*(4), 520.
- (28) Park, K.; Lee, Y.; Lee, J.; Lim, S. *Appl. Surf. Sci.* **2008**, *254*, 4828.
- (29) Adhikari, H.; McIntyre, P. C.; Sun, S.; Pianetta, P.; Chidsey, C. E. D. *Appl. Phys. Lett.* **2005**, *87*, 263109.
- (30) Jagannathan, H.; Kim, J.; Deal, M.; Kelly, M.; Nishi, Y. *ECS Trans.* **2006**, *3*(7), 1175.

- (31) Scheres, L.; Giesbers, M.; Zuilhof, H. *Langmuir* **2010**, *26*(7), 4790.
- (32) Cicero, R. L.; Linford, M. R.; Chidsey, C. E. D. *Langmuir* **2000**, *16*, 5688.
- (33) Webb, L. J.; Lewis, N. S. *J. Phys. Chem. B* **2003**, *107*, 5404.
- (34) Sharp, I. D.; Schoell, S. J.; Hoeb, M.; Brandt, M. S.; Stutzmann, M. *Appl. Phys. Lett.* **2008**, *92*, 223306.
- (35) Choi, K.; Buriak, J. M. *Langmuir* **2000**, *16*(20), 7737.
- (36) Boe, A.; Nguyen, S. T.; Kim, J.-H. *Nanoscope* **2008**, *5*(1), 124.
- (37) Park, K.; Lee, Y.; Im, K. T.; Lee, J. Y.; Lim, S. *Thin Solid Films* **2010**, *518*(15), 4126.
- (38) Holmberg, V. C.; Korgel, B. A. *Chem. Mater.* **2010**, *22*(12), 3698.
- (39) He, J.; Lu, Z. H.; Mitchell, S. A.; Wayner, D. D. M. *J. Am. Chem. Soc.* **1998**, *120*, 2660.
- (40) Vegunta, S. S. S.; Ngunjiri, J. N.; Flake, J. C. *Langmuir* **2009**, *25*(21), 12750.
- (41) Bashouti, M. Y.; Stelzner, T.; Christiansen, S.; Haick, H. *J. Phys. Chem. C* **2009**, *113*, 14823.
- (42) Bashouti, M. Y.; Stelzner, T.; Berger, A.; Christiansen, S.; Haick, H. *J. Phys. Chem. C* **2008**, *112*(49), 19168.
- (43) Loscutoff, P. W.; Bent, S. F. *Annu. Rev. Phys. Chem.* **2006**, *57*, 467.
- (44) Kosuri, M. R.; Cone, R.; Li, Q. M.; Han, S. M.; Bunker, B. C.; Mayer, T. M. *Langmuir* **2004**, *20*(3), 835.
- (45) Han, S. M.; Ashurst, R.; Carraro, C.; Roy, M. *J. Am. Chem. Soc.* **2001**, *123*, 2422.
- (46) Ardalani, P.; Musgrave, C. B.; Bent, S. F. *Langmuir* **2009**, *25*, 2013.
- (47) Ngo, L. T.; Almécija, D.; Sader, J. E.; Daly, B.; Petkov, N.; Holmes, J. D.; Ert, D.; Boland, J. J. *Nano Lett.* **2006**, *6*, 2964.

The reactions were carried out at a temperature and pressure of 400 °C and 24.1 MPa, respectively, yielding nanowires with a mean diameter of 80 nm. The nanowires displayed a predominately $\langle 111 \rangle$ growth direction with $\langle 110 \rangle$ and $\langle 112 \rangle$ growth directions also present.

Diethyl ether (Et_2O) was distilled from Na/benzophenone; anhydrous methanol (MeOH) and isopropyl alcohol (IPA) were purchased from Sigma-Aldrich. All other reagents were purchased from Sigma-Aldrich. Halogen termination of the Ge nanowires was carried out by immersing the nanowires into 10% aqueous HCl and HBr and 5% aqueous HI solutions for 10 min. The substrates were washed with deionized water and IPA and dried under N_2 . The Ge nanowires were functionalized with alkyl chains via a halogenation/alkylation route using alkyl Grignard reagents. After halogen passivation, the nanowires were immersed in 1 M dodecylmagnesium bromide (DD-MgBr) in Et_2O and heated to 45 °C for 24–72 h. The substrates were soaked in anhydrous Et_2O for 5 min and then rinsed with more Et_2O . This soaking/rinsing procedure was repeated three times. The nanowires were then rinsed with MeOH and dried under N_2 . Ge nanowires were passivated with alkanethiols by immersion into 0.1 M dodecanethiol in anhydrous IPA. The nanowires were heated to 60 °C for 2–24 h under N_2 . Following the passivation procedure, the substrates were soaked in IPA for 5 min and rinsed with IPA ($\times 3$). The nanowires were then rinsed with chloroform and MeOH and dried with N_2 .

Characterization of Functionalized Ge Nanowires. Scanning electron microscopy (SEM) images were acquired on a FEI Inspect F, operating at 5 kV accelerating voltage. Transmission electron microscopy (TEM) images were acquired using Jeol 2010 at 200 kV accelerating voltage. Attenuated total reflectance infrared (ATR-IR) spectra were recorded on a PerkinElmer Spectrum 100 using 20 scans with 2 cm^{-1} resolution. The nanowires were dispersed in tetrachloromethane and dropped onto the ATR crystal (ZnSe). The solvent was allowed to dry before the measurements were recorded. X-ray photoelectron spectroscopy (XPS) analysis was conducted on a VSW Atom Tech System using achromatic Al X-rays with a twin anode (Al/Mg) X-ray source. Survey spectra were captured at a pass energy of 100 eV, a step size of 0.7 eV, and dwell time of 0.1 ms. The core level spectra obtained were averaged over 15 scans and captured at a pass energy of 50 eV, a step size of 0.2 eV, and a dwell time of 0.1 ms. XPS data was also acquired using a KRATOS AXIS 165 monochromatized X-ray photoelectron spectrometer equipped with a dual anode (Mg/Al) source. Survey spectra were captured at a pass energy of 100 eV, step size of 1 eV, and dwell time of 50 ms. The core level spectra were an average of 10 scans captured at a PE of 25 eV, step size of 0.05 eV, and dwell time of 100 ms. The spectra were corrected for charge shift to the C 1s line at a binding energy of 284.6 eV. A Shirley background correction was employed, and the peaks were fitted to Voigt profiles. The Ge 3d signals were fitted to two peaks with a spin–orbit coupling of 0.58 eV and an intensity ratio of 3:2, corresponding to the Ge $3d_{5/2}$ and Ge $3d_{3/2}$, respectively. In Figure 1, the Ge oxide peaks were plotted by adding separate peak contributions using Gaussian profiles. The peaks were centered at 30.5, 31.35, 32.2, and 33.05 eV, corresponding to Ge^{1+} , Ge^{2+} , Ge^{3+} , and Ge^{4+} , respectively.¹⁶ The S 2p doublet peaks were fitted to Voigt profiles with a spin–orbit splitting of 1.2 eV.⁴⁸ XPEEM measurements were carried out at the

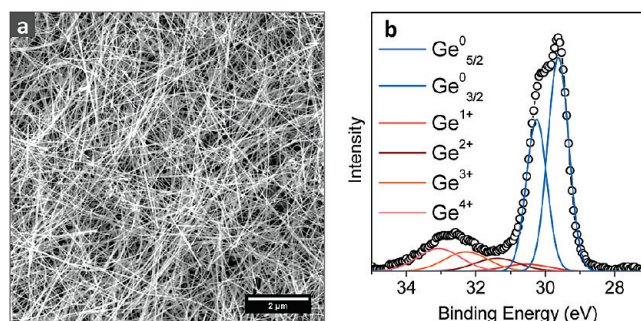


Figure 1. (a) SEM image of Ge nanowires grown in sc-toluene at a temperature of 400 °C and pressure of 24.1 MPa from a Au-coated Si substrate and (b) the corresponding Ge 3d XPS core level spectra of the Ge nanowires acquired 1 week after synthesis.

nanospectroscopy beamline at the Elettra synchrotron facility in Trieste, Italy. A detailed description of the beamline setup is described elsewhere.^{49,50} The passivated nanowires were dispersed in IPA and drop cast onto doped Si substrates. Ge nanowire passivation was carried out by immersion into aqueous halide acid solutions. The substrates were rinsed with deionized water and methanol and dried under Ar.

Results and Discussion

Relative Stability of Halogenated Ge Nanowires.

Figure 1a shows a SEM image of Ge nanowires synthesized on a Au-coated Si substrate. Once removed from the reaction vessel, the surface of the nanowires begins to oxidize immediately. The Ge 3d XPS core level spectra shown in Figure 1b is composed of an elemental Ge peak, which exhibits spin–orbit splitting of 0.585 eV, consistent with that of the Ge $3d_{5/2}$ and Ge $3d_{3/2}$ peaks, located at 28.6 and 29.2 eV, respectively.¹⁶ In addition to bulk Ge, four chemically shifted satellite peaks at higher binding energies are also present, corresponding to the four Ge surface oxidation states, as illustrated in Figure 1b.

Oxide removal and halogen termination was achieved by treatment with aqueous halide solutions. Jagannathan et al.³⁰ previously used 20% HBr and HI solutions for generating halogen-terminated Ge nanowires. However, we observed considerable roughening of the Ge nanowire surfaces at these concentrations, and consequently, 10% HCl or HBr solutions were used in our study. A 10% HI solution was found to be particularly aggressive to our nanowires, etching both the surface oxide and the crystalline Ge (with a known etching rate of 0.6 nm min^{-1}),⁵¹ leading to very rough surfaces, as shown in figure S1 in the Supporting Information. Rough surfaces have been demonstrated to oxidize faster than smooth surfaces, and consequently, a 5% HI solution was used in our studies.²⁸

(48) Cavalleri, O.; Gonella, G.; Terreni, S.; Vignolo, M.; Pelori, P.; Floreano, L.; Morgante, A.; Canepa, M.; Rolandi, R. *J. Phys.: Condens. Matter* **2004**, *16*(26), S2477.

(49) Schmidt, T.; Heun, S.; Slezak, J.; Diaz, J.; Prince, K. C.; Lilienskamp, G.; Bauer, E. *Surf. Rev. Lett.* **1998**, *6*, 1287.

(50) Locatelli, A.; Bianco, A.; Cocco, D.; Cherifi, S.; Hein, S.; Marsi, M.; Pasqualetto, M.; Bauer, E. *J. Phys. IV* **2003**, *104*, 99.

(51) Onsia, B.; Conard, T.; De Gendt, S.; Heynes, M.; Hofliijk, I.; Mertens, P.; Meuris, M.; Raskin, G.; Sioncke, S.; Teerlinck, I.; Theuwis, A.; Van Steenberghe, J.; Vinckier, C. *Solid State Phenom.* **2005**, *103*, 267.

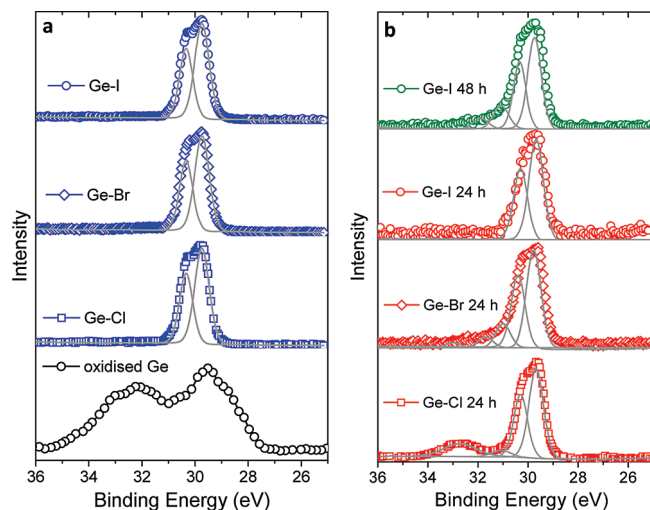


Figure 2. Ge 3d XPS core level spectra showing (a) Ge nanowires immediately after treatment with HCl, HBr, and HI and (b) iodide-terminated Ge nanowires after 48 h ambient exposure and chlorine-, bromine-, and iodine-terminated Ge nanowires after 24 h ambient exposure.

Figure 2 compares the Ge 3d XPS core level spectra of halogen-terminated nanowires after immediate treatment and after ambient exposure ($\sim 20^\circ\text{C}$, 70% relative humidity). All halide solutions effectively removed the surface oxide, as illustrated by the absence of oxide associated peaks in the spectra immediately after acid treatment (blue spectra). After 24 h exposure to air (red spectra), the Cl-terminated nanowires showed the greatest degree of Ge reoxidation, the HBr treated nanowires displayed only minor oxide formation, and the HI treated nanowires showed no reoxidation of the surface. The I-terminated surfaces exhibited a small oxide peak after 48 h ambient exposure. The stability of halogenated Ge surfaces increased with the increasing size of the halogen species ($\text{Cl} < \text{Br} < \text{I}$), as the larger halogen atoms serve as a better steric barrier to prevent reoxidation of the surface. Differences in the electronegativity of the halogen species also influences the reactivity of the halogen-terminated Ge surfaces.⁵² Electronegativity values decrease down Group 17 in the periodic table, and consequently, the electronegativity difference between Ge and the halogen species reduces from Ge–Cl (1.5) to Ge–Br (0.95) to Ge–I (0.65),⁵³ leading to a higher degree of covalent bonding. Furthermore, the increasing orbital size of Cl (2p), Br (3p), and I (4p) means that the length of the Ge–X bond increases from $\text{Cl} < \text{Br} < \text{I}$. The combined effect of a weaker bond, longer bond length, and smaller electronegativity difference reduces the Ge–X bond polarization with increasing halogen size, i.e., $\text{X} = \text{Cl} > \text{Br} > \text{I}$.⁵² Less polarized Ge–X bonds are, thus, more resistant to an oxidative nucleophilic attack from O_2 and H_2O species, thereby giving larger halogen species greater stability on the Ge surface.

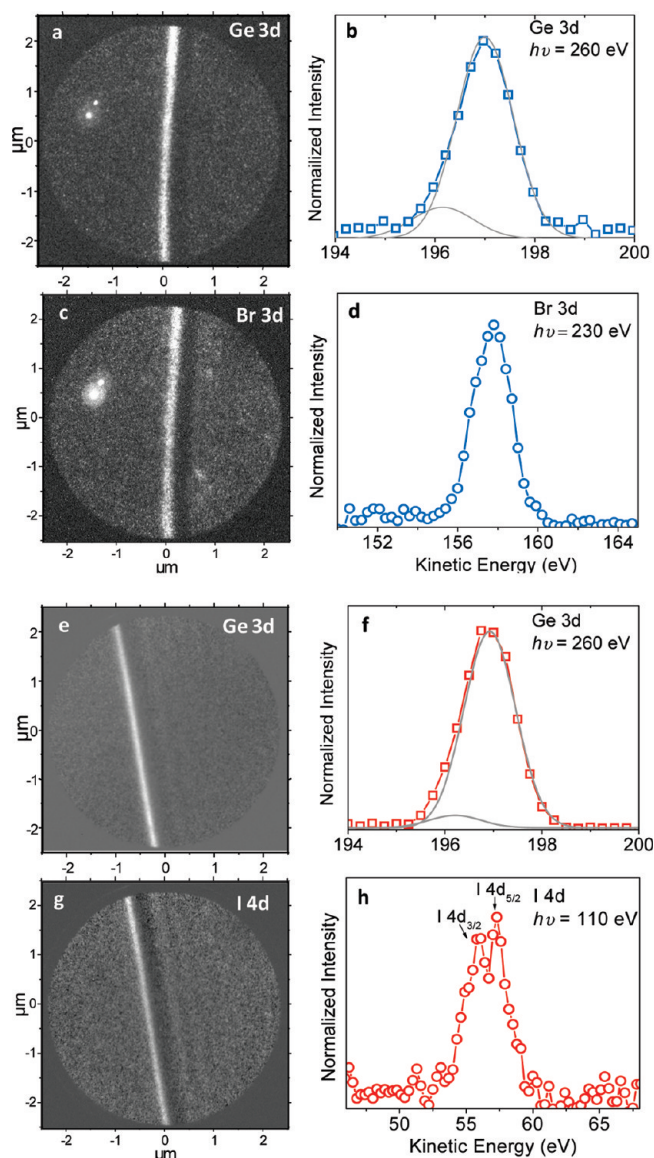


Figure 3. XPEEM images and spectra of (a–d) bromine-terminated nanowires, illustrating the Ge 3d and Br 3d spectra, and (e–h) iodine-terminated Ge nanowires, illustrating the Ge 3d and I 4p spectra.

XPEEM Analysis of Individual Bromine and Iodine Passivated Ge Nanowires. Figure 3a–h illustrates XPEEM images and the corresponding background-subtracted, normalized Ge 3d and Br 3d spectra. The presence of Br species on the nanowire surface is clearly observed in the Br 3d PEEM image, Figure 3c. Furthermore, the Ge 3d spectra of the bromine-terminated nanowire exhibits a shoulder peak shifted to a lower kinetic energy, which is consistent with Ge bonding to the more electronegative Br atom.⁴⁶ The Ge 3d spectra of the iodine-terminated nanowire, shown in Figure 3e, is best fitted with two peaks, one corresponding to Ge and the other chemically shifted by 0.4 eV due to the presence of iodine species. The presence of an iodine-terminated surface is also indicated by the I 4d XPEEM image and corresponding I 4d spectra shown in Figure 3g,h, respectively.

The halogen surface coverage can be estimated from the integral intensities of the Ge and halogen XPEEM spectra. The intensities were corrected for spectra that

(52) Kachian, J. S.; Wong, K. T.; Bent, S. F. *Acc. Chem. Res.* **2010**, 43(2), 346.

(53) *CRC Handbook of Chemistry and Physics*; CRC Press: Boca Raton, FL, 1994; Vol. 75th ed.

were collected at different photon energies. A detailed description of the XPEEM data analysis is described elsewhere.^{54,55} The monolayer surface coverage (θ_x) was estimated from eq 1:

$$\theta_x = \frac{I_x/\sigma_x}{(I_x/\sigma_x) + (I_{\text{Ge}}/\sigma_{\text{Ge}})} \quad (1)$$

where I_x and I_{Ge} are the integrated intensities of the Ge and halogen species, respectively, and σ_x and σ_{Ge} are the corresponding photoionization cross sections taken from literature values.⁵⁶ The estimated values for θ_{Br} and θ_{I} were found to be 1.04 and 0.91, respectively. The surface coverage values were an average of six Br-terminated and five I-terminated nanowires with a standard deviation of 0.09 and 0.13, respectively. It must be noted that errors such as nonlinear background and approximations in photoemission cross sections introduce errors into the surface coverage calculations, estimated to be ± 0.2 . The surface halogen coverage suggests complete termination after HBr/HI treatment, which corresponds to literature studies on planar Ge surfaces.^{15,46} However, it is difficult to draw conclusions by comparison with studies on planar surfaces as the Ge nanowires possess a predominate $\langle 111 \rangle$ growth direction, having $\{110\}$ surface facets. In contrast to Ge(100) and Ge(111) planar surfaces, the Ge(110) surface has been much less investigated. The halogen coverage may also be less than unity if dihalide species are present on the nanowire surfaces.

Alkylation and Thiolation of Halogen-Terminated Ge Nanowires. Figure 4 illustrates XPS spectra of Cl-terminated Ge nanowires as well as alkane and alkanethiol functionalized nanowires, obtained via chlorinated surfaces. After alkylation with DD-MgBr, there was an increase in the intensity of the C 1s peak relative to the chlorinated nanowires. The presence of carbon in the untreated and halogen-terminated nanowires can be attributed to adventitious hydrocarbons adsorbed onto their surfaces and residual carbon contamination from the nanowire synthesis. Furthermore, the absence of the Mg 2p (50 eV) and Br 3d (70 eV) peaks in the spectra is suggestive that the alkyl chains are covalently attached and not merely adsorbed onto the Ge nanowire surfaces. After reacting the Cl-terminated Ge nanowires with Grignard reagents for 24 h, Cl species were still observed in the XPS survey, as shown by the presence of the Cl 2s and Cl 2p peaks at binding energies of 269 and 200 eV, respectively (Figure 4a). After 48 h, there was a reduction in the intensity of the Cl 2s peak; however, complete removal of Cl species on the alkylated surfaces was not achieved. The high resolution Cl 2s spectrum shown in Figure 4b, taken after a reaction time of 72 h, indicates that some Cl atoms still remain on the nanowire surfaces.

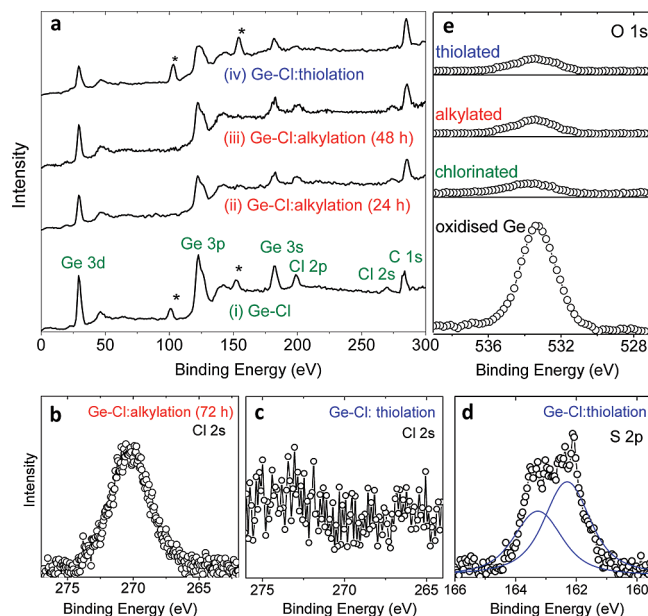


Figure 4. (a) XPS survey scans of Cl-terminated Ge nanowires and alkylation and thiolation functionalization via chlorinated surfaces, (b) Cl 2s core-level spectrum showing the presence of Cl after an alkylation reaction time of 72 h, (c) Cl 2s core-level spectrum after thiol functionalization, (d) S 2p core-level spectrum after thiolation reaction, (e) O 1s core level spectra of Ge nanowires before and after surface functionalization. The asterisks mark signals from the Si wafer.

There was no change in the intensity of Ge 3d/Cl 2s XPS peaks after alkylation times > 72 h. In comparison to alkylation, thiolation reactions on chlorinated Ge surfaces showed no Cl species in the XPS analysis after a reaction time of 4 h, as shown in the high resolution Cl 2s spectrum in Figure 4c. Figure 4d displays the high resolution S 2p XPS core level spectrum of the thiolated nanowires centered at 162.7 eV, which is in good agreement with binding energies reported for thiolated monolayers.^{57–59}

Figure 4e illustrates the O 1s XPS core level spectra for oxidized, chlorinated, alkylated, and thiolated nanowires. After HCl treatment, the intensity of the oxide peak was reduced considerably due to the removal of GeO_x , but a small oxide signal remained which can be mainly attributed to the presence of adsorbed molecules after aqueous HCl treatment and from the MeOH rinse. Although the Ge 3d spectra indicated an oxide free surface, reports on planar surfaces have shown that trace amounts of oxide are not always observed in the Ge 3d spectra and can be detected in the Ge 2p spectra, which is more surface sensitive.¹⁷ After alkylation and thiolation, there is a slight increase in the intensity of the O (1s) peak, most likely attributed to oxygen functionalities in the solvents used for the functionalized reactions (IPA, Et_2O). Reactions of thiols at the Ge surface are more favorable than alcohols due to the lower S–H bond dissociation energy compared to that of the O–H bond.⁵²

(54) Ratto, F.; Locatelli, A.; Fontana, S.; Kharrazi, S.; Ashtaputre, S.; Kulkarni, S. K.; Heun, S.; Rosei, F. *Small* **2006**, 2(3), 401.

(55) Ratto, F.; Rosei, F.; Locatelli, A.; Cherifi, S.; Fontana, S.; Heun, S. *J. Appl. Phys.* **2005**, 97, 043516.

(56) Yeh, J. J.; Lindau, I. *At. Nucl. Data Tables* **1985**, 32(1), 1.

(57) Jun, Y.; Zhu, X. Y.; Hsu, J. W. P. *Langmuir* **2006**, 22(8), 3627.

(58) Desikan, R.; Armel, S.; Meyer, H. M.; Thundat, T. *Nanotechnology* **2007**, 18, 42.

(59) Ardalan, P.; Sun, Y.; Pianetta, P.; Musgrave, C. B.; Bent, S. F. *Langmuir* **2010**, 26(11), 8419.

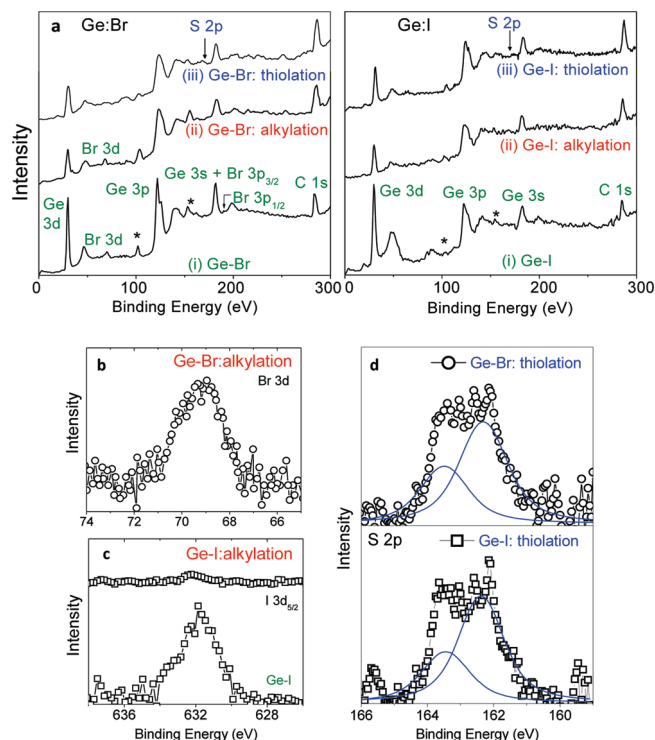


Figure 5. (a) XPS survey spectra of Ge nanowire functionalization on Br- and I-terminated surfaces. (b) Br 3d spectra after alkylation. (c) The I 3d spectra before and after iodinations. (d) The S 2p spectra after thiolation of Br- and I-terminated surfaces.

Figure 5a shows XPS survey scans of brominated and iodinated Ge nanowires as well as functionalization of these halogenated surfaces with Grignards and alkanethiols. Bromination of the Ge surface can be seen from the presence of the Br 3d peak located at a binding energy of 69.1 eV. Alkylation and thiolation on Br and I surfaces are both accompanied by an increase in their respective C 1s signal. After alkylation, there is a reduction but not a complete disappearance of the halogen species, similar to the trend observed on Cl-terminated surfaces. The position of the Br 3d peak at 69.1 eV in Figure 5b is consistent with Br bonded to a Ge surface; if the Br peak was due to unreacted Grignard reagent, i.e., DD-MgBr, the Br 3d peak would be observed at a lower binding energy, as Br bonded to a more electropositive Mg atom (electronegativity (en) = 1.3) would undergo a larger chemical shift, relative to Ge (en = 2.0).⁵³ Figure 5c shows the I 3d_{5/2} peak at a binding energy of 632 eV, after HI treatment as well as an I signal after alkyl functionalization. Thiolation of Br- and I-terminated surfaces was accompanied by the appearance of the S 2p peak shown in Figure 5d and the absence of any Br and I peaks in the XPS spectra.

The absence of halogen species in the XPS survey spectra, after thiol functionalization, indicates that alkanethiols are more effective in replacing surface halogen species compared to alkyl Grignard reagents. After ~72 h of immersion in the Grignard solution, there is negligible change in the intensity of the Ge/halogen XPS peaks, indicating that further reaction with the remaining halogen species is unfavorable. The mechanism for

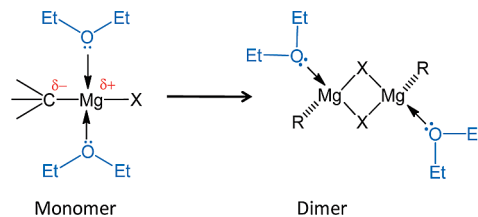
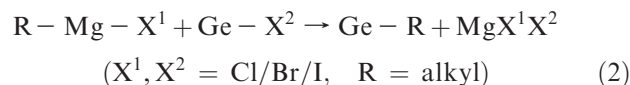


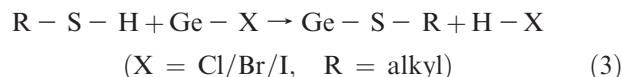
Figure 6. Schematic illustrating the coordination of solvent molecules to Grignard reagents.

the covalent attachment of Grignard reagents to Ge surfaces is illustrated in eq 2.



Grignard reagents are extremely reactive species due to a highly nucleophilic carbon atom adjacent to the Mg atom; consequently, the reduced reactivity toward halogen-terminated Ge surfaces may be due to steric constraints. Both DDT and DD-MgBr have similar chain lengths (~18 Å) and only differ in the nature of their functional head groups. While Grignard reagents are commonly noted as “R–MgX” ($\text{X} = \text{Cl}, \text{Br}, \text{I}$), their actual structure in solution is described by the Schlenk equilibrium which involves the coordination of solvent molecules to the Mg atom.⁶⁰ Furthermore, ethereal solutions of Grignard reagents in a concentration range of 0.5–1 M exist as dimeric complexes, as illustrated in Figure 6.⁶¹

The mechanism for thiolation involves abstraction of the surface halogen to form a corresponding hydrogen halide, as shown in eq 4⁶ 3:



Although alkylation is carried out at a lower temperature than thiolation (45 °C versus 60 °C) which can be expected to influence the reaction kinetics, increased steric effects experienced by Grignard reagents due to solvent coordination may also hinder the ability to access the halogenated species on the nanowire surface, consequently resulting in unreacted residual halogen species detected by XPS analysis.

ATR-IR and TEM Analysis of Functionalized Ge Nanowires. Figure 7 shows ATR-IR spectra of DD-functionalized (red spectra) and DDT-functionalized (blue spectra) Ge nanowires via modification of the initially Cl-, Br-, and I-terminated nanowire surfaces. Stretching vibrational modes associated with aliphatic alkyl chains are visible for all samples (2800–3000 cm^{-1}), further indicating that the Grignard reagents and alkanethiols have reacted with the halogen-terminated Ge surfaces. The ATR-IR spectra of alkanethiol passivated nanowires, Figure 7b, show essentially identical absorbance frequencies for Cl-, Br-, and I-terminated surfaces.

(60) Silverman, G. S.; Rakita, P. E. *Handbook of Grignard Reagents*; Marcel Dekker Inc.: New York, 1996.

(61) Asbey, E. C.; Smith, M. J. *J. Am. Chem. Soc.* **1964**, 86(20), 4363.

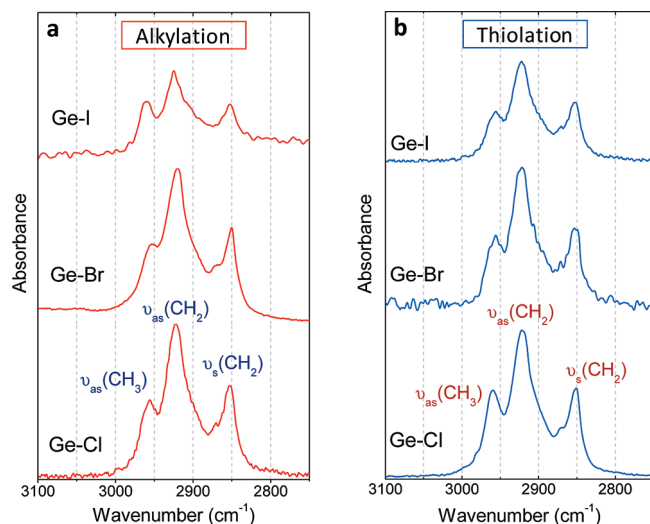


Figure 7. ATR-FTIR spectra of (a) dodecyl- and (b) dodecanethiol-functionalized Ge nanowires from Cl-, Br-, and I-terminated surfaces.

The C–H asymmetric and symmetric stretches are observed at 2921 and 2851 cm^{-1} , respectively, while the asymmetric CH_3 absorption peak is observed at 2955 cm^{-1} . These peak positions are in good agreement with IR absorbance frequencies reported by Kosuri et al.⁴⁴ for alkanethiol functionalized bulk Ge surfaces. The peak positions of the C–H stretching modes occur at lower frequencies relative to isotropic liquid DDT, indicating that a degree of crystalline order is present in the alkanethiol passivation layer.^{38,62,63} For Ge nanowires alkylated from Cl- and Br-terminated surfaces, the symmetric and asymmetric CH_2 stretching modes occur at 2921 and 2852 cm^{-1} , similar to those on thiolated surfaces. The asymmetric CH_2 stretching mode of highly crystalline hydrocarbons typically appears at 2918 cm^{-1} ,⁶² suggesting that some disorder is present in the alkyl and thiol functionalization layers. The vibrational modes for alkylation via I-terminated surfaces exhibited the highest absorption frequencies ($\nu_{\text{as}}\text{CH}_2$: 2924 cm^{-1} , $\nu_{\text{a}}\text{CH}_2$: 2853 cm^{-1} , $\nu_{\text{a}}\text{CH}_3$: 2959 cm^{-1}), indicating the most disordered passivation layer was achieved via a iodination/alkylation route. The presence of unreacted halogen species or defects at the nanowire surface would be expected to disrupt the ordering and assembly of the passivating ligands.

Figure 8a–c displays SEM images of Ge nanowires before and after surface passivation and shows that the morphologies of the nanowires were not altered by the functionalization procedures. Figure 8d–f shows TEM images of Ge nanowires before and after functionalization. The native Ge oxide (GeO_x), typically $\sim 2\text{--}4\text{ nm}$, shown in Figure 8d has been replaced by a thin passivation layer ($\sim 1.8\text{ nm}$) composed of the alkane and alkanethiol ligands, Figure 8e,f, respectively. TEM analysis showed little difference between the thicknesses of the passivation layer formed from different halogen-terminated surfaces.

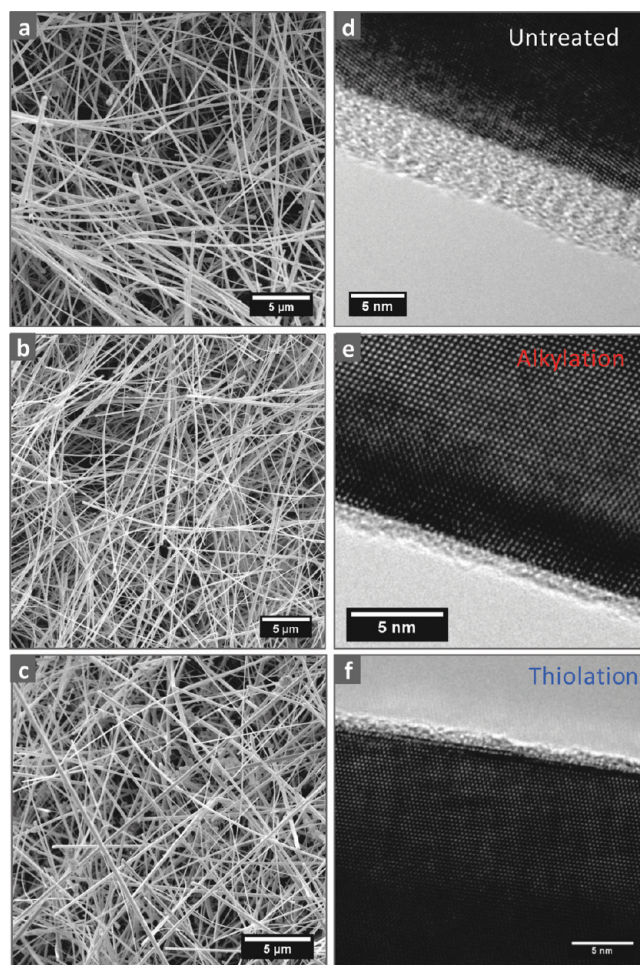


Figure 8. SEM and TEM images of Ge nanowires (a, c) post functionalized, (b, e) alkylated with DD-MgBr, and (c, f) thiolated with DDT.

Stability of Alkyl and Alkanethiol Passivation Layers: Influence of Halogen Species. The degree of reoxidation of the Ge surface provides insight into the quality of the passivation monolayers attained from the halogenated surfaces. Figure 9a,b illustrates the XPS Ge 3d peaks for Cl/Br/I surfaces functionalized with alkyl and alkanethiols, respectively, after 1 week exposure to ambient conditions. Overall, Ge nanowires functionalized with DD chains via Grignard reagents (red spectra) display a higher degree of reoxidation compared to DDT (blue spectra) passivated surfaces, as indicated by the greater oxide component in the Ge 3d spectra. A comparison of the spectra within Figure 8a shows that alkyl passivation via chlorinated surfaces exhibit the most oxidation, while passivation via iodinated surfaces shows the least. The opposite trend is observed for alkanethiol passivation, with Ge nanowires thiolated from Cl- and Br-terminated surfaces showing no oxidation after ambient exposure for 1 week, while thiolation via iodinated surfaces do exhibit some reoxidation. The oxide shifted peak in the Ge 3d XPS core level spectrum is small, indicating only minor oxidation of the surface.

The stability trend observed for alkylated ($\text{Cl} < \text{Br} < \text{I}$) and thiolated ($\text{I} < \text{Br} \approx \text{Cl}$) Ge nanowire surfaces can be explained as follows. Thiolation of halogenated surfaces results in the complete removal of the halogen atoms, but

(62) Bensebaa, F.; Voicu, R.; Huron, L.; Ellis, T. H.; Kruus, E. *Langmuir* **1997**, *13*, 5335.

(63) Linford, M. R.; Fenter, P.; Eisenberger, P. M.; Chidsey, C. E. D. *J. Am. Chem. Soc.* **1995**, *117*, 3145.

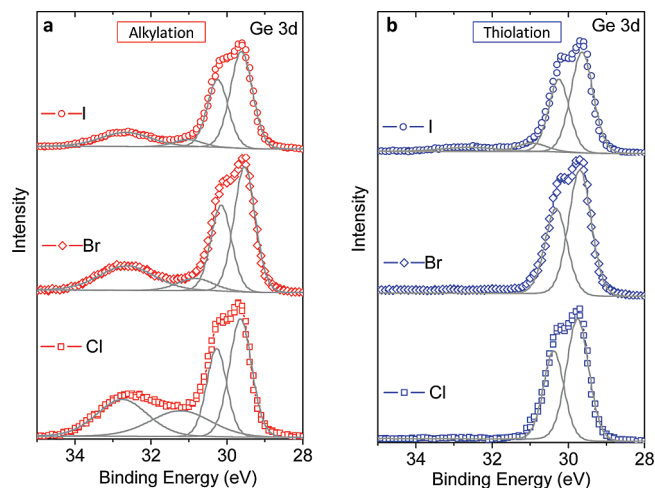


Figure 9. Ge 3d XPS core level spectra of (a) dodecyl functionalized Ge nanowires and (b) dodecanethiol functionalized Ge nanowires after exposure to ambient conditions for 1 week.

alkylation via Grignard reagents does not; therefore, the stability of the halogen species must also be considered for the alkylated surfaces. The residual halogen atoms on the surface are more susceptible to oxidation than alkylated surfaces, which are more hydrophobic. In addition, the long hydrocarbon chain length serves as a better steric barrier from atmospheric O_2/H_2O compared to single halogen species, and the covalent character of the bond prevents bond cleavage. Furthermore, the Ge–C bond strength is 460 kJ mol^{-1} , which is greater than Ge–X (where $X = \text{Cl}$ (356 kJ mol^{-1})/Br (276 kJ mol^{-1})/I (213 kJ mol^{-1})).⁵³ As illustrated in Figure 2, the stability of halogen termination increases with the heavier atom; consequently, the observed trend in alkyl stability parallels that of the halogen stability, i.e., $\text{Cl} < \text{Br} < \text{I}$. The residual halogen species prevents the formation of densely packed monolayers, allowing for oxidizing species to readily gain access to the nanowire surface, and consequently, alkylated surfaces are considerably more oxidized after 1 week than the thiolated samples.

Thiolation on all halogen-terminated Ge surfaces provides relatively good stability (over 1 week), with minor oxidation observed only on nanowires thiolated from iodated surfaces. The Ge–I bond is much less polarized than the Ge–Cl/Br bonds, giving rise to a higher activation energy barrier for alkanethiol attachment; consequently,^{46,59} alkanethiol formation from iodated surfaces is less favorable than chlorinated and brominated Ge surfaces.

Although thiolation on halogenated Ge nanowires has not been reported, several studies of thiolation via hydrogen-terminated surfaces have found thiols to provide better protection against surface reoxidation compared to alkyl chains.^{18,64,65} In this study, it is evident from Figure 9 that thiol functionalization of halogenated surfaces also display greater stability than alkyl functionalization. Interestingly, literature reports on planar Ge surfaces found that alkyl

ligands (Ge–C) impart greater passivation than alkanethiol ligands (Ge–S).⁴⁵ Although there have been no literature studies into the origin of this trend, high surface curvature, surface roughness, and the presence of defects are all likely to have some influence on the stability of passivation layer on nanowire surfaces compared to planar surfaces.

Conclusions

In summary, the surface halogenation of Ge nanowires with Cl, Br, and I atoms, followed by surface functionalization with alkanes and alkanethiols, was investigated. The stability of the halogenated surfaces of the Ge nanowires increased from $\text{Cl} < \text{Br} < \text{I}$ due to the increasing size of the heavier halogen atom which provided a greater steric barrier to oxidative attack. Attachment of dodecyl chains via Grignard reagents did not result in complete removal of the surface halogens, even after long reaction times. Conversely, after thiolation of the nanowire surfaces, no halogen species were detected by XPS. Greater steric constraints due to dimerization and solvent coordination associated with alkyl Grignard reagents are attributed to the reduced reactivity of alkyl functionalization compared to alkanethiols. Incomplete surface functionalization via Grignard reagents was also reflected in stability studies of the alkane and alkanethiol functionalized nanowires. After exposure to ambient conditions for 1 week, the alkylated nanowires showed a greater degree of reoxidation relative to thiolated nanowire surfaces. Furthermore, nanowires alkylated via chlorinated surfaces displayed the greatest degree of Ge oxidation while alkylation via iodated surfaces exhibited the least, a trend which reflects the stability of the residual halogen species on the nanowire surface upon alkylation. On the other hand, alkanethiol passivation layers showed excellent ambient stability; functionalization from Cl and Br surfaces showed no reoxidation of the surface after 1 week, while those formed from iodated surfaces only exhibited minor oxidation. Overall, the results show that alkanethiol functionalization of Ge nanowires can be achieved from halogenated surfaces and that the stability of these passivation layers exceeds that of alkyl layers formed from Grignard reagents.

Acknowledgment. We acknowledge financial support from the Irish Research Council for Science, Engineering, and Technology (IRCSET) and Science Foundation Ireland (Grant 08/CE/I1432). This research was also enabled by the Higher Education Authority Program for Research in Third Level Institutions (2007–2011) via the INSPIRE programme. The authors are grateful to the researchers at the Trieste Synchrotron Facility, Italy, for their assistance with XPEEM measurements and Michael Schmidt in the Electron Microscopy and Analysis Facility (EMAF) at the Tyndall National Institute, Ireland, for help with HRTEM imaging.

Supporting Information Available: TEM image illustrating the surface roughness of Ge nanowires as a result of etching with 10% HI. Estimation of surface coverage on alkylated Ge nanowires from XPS data (PDF). This material is available free of charge via the Internet at <http://pubs.acs.org>.

(64) Wang, D.; Dai, H. *Appl. Phys. A: Mater. Sci. Process.* **2006**, *85*, 217.

(65) Wang, D.; Chang, Y.-L.; Liu, Z.; Dai, H. *J. Am. Chem. Soc.* **2005**, *127*, 11871.